

**Original Article**

## Screening and Docking Molecular Studies of Natural Products Targeting overexpressed Receptors HER-2 in Breast Cancer

Nesrine Lenchi<sup>1,2\*</sup>, Naima Maouche<sup>1</sup>, Souad Khemili-Talbi<sup>2</sup>

1. Department of Natural and Life Sciences, Faculty of Sciences, University Algiers 1 BenYoucef Benkhedda, Algiers, Algeria

2. Department of Microbiology and Biomolecules, Faculty of Sciences, University of M'Hamed Bougara of Boumerdès, Algeria.

**Article Info:**

**Received:** 27 June 2024

**Revised:** 20 September 2024

**Accepted:** 23 September 2024

**Keywords:**

Breast Cancer,  
HER-2, Molecular Docking,  
Natural Compounds.

### ABSTRACT

Breast cancer is the first cancer to affect a community. Because of its extremely high mitotic activity, breast cancer that tests positive for HER 2 is considered to have a poor prognosis. Due to the side effects of chemical drugs, patients are increasingly turning to natural medicine, such as phytotherapy and nutritherapy. The study uses a bioinformatics approach (molecular docking) to search for new, non-toxic anti-cancer inhibitors. The study screens 102 ligands from natural and dietary compounds that are likely to interact with the HER-2. The virtual screening results allow us to select the 23 best compounds which can be proposed as the most effective HER-2 inhibitors. Lycopene would be a very promising ligand which presents a DeltaG of -9.82 kcal/mol. Other promising ligands include beta-carotene (DeltaG of -8.58), P-cumaric acid kcal/mol (DeltaG of -8.57) and Curcumin (DeltaG of -8.46). Other compounds, luteolin, anacardium (Anacardic acid) and alpha-Tocopherol, were found to have the strongest inhibitory effects with DeltaG values of -7.92 kcal/mol, -7.89 kcal/mol, and -7.85 kcal/mol, respectively. These compounds act directly on residues keys found in the hydrophobic pocket II (ATP binding site) and the hydrophobic region (the  $\alpha$ C- $\beta$ 4 loop) of the EGFR domain. Pinoresinol, Kaempferol and Caffeic acid have DeltaGs of -7.48 Kcal/mol, -6.88 Kcal/mol and -6.34 kcal/mol, respectively. These three ligands are specific to the conserved regions of the HER-2 receptor and interact with the C-terminal, the C-lobe activation loop and the N-lobe P loop of the tyrosine kinase domain, respectively. Lapatinib (chemical compound) and quercetin (natural compound) have DeltaG of -7.58 kcal/mol and -7.28 kcal/mol, respectively, form a hydrogen bond with the same residue in the hydrophobic region. All the natural molecules seem very promising and, after *in vitro/in vivo* tests, could constitute good substitutes for the chemotherapies which are currently used to treat breast cancers as well as other cancers.

**Corresponding Author:**

**n.lenchi@univ-alger.dz**



**How to cite this article:** Lenchi N, Maouche N, Khemili-Talbi S. Screening and Docking Molecular Studies of Natural Products Targeting overexpressed Receptors HER-2 in Breast Cancer. *Archives of Razi Institute*. 2025;80(3):721-733. DOI: 10.32592/ARI.2025.80.3.721



## 1. Introduction

Breast cancer is the second most common malignancy and the second leading cause of cancer-related deaths in women (1). In early 2020, the World Health Organization (WHO) announced the incidence of breast cancer is rising in developing nations due to rising life expectancies, increased urbanization, and the adoption of Western lifestyles. It is estimated that 627,000 women died of breast cancer in 2020, accounting for 15% of all female cancer deaths. Estrogen and progesterone hormone receptor dysfunction is typically associated with breast tumors (2, 3). Furthermore, a great deal of research has been conducted on the overexpression of the human epidermal growth factor receptor 2 (HER2), overexpression of the epidermal growth factor receptor (EGFR1), and PI3Ka (dysregulation of the ER+ and ER-) signaling pathways in breast cancer (3, 4).

Therefore, it is essential to discover novel techniques and compounds that target these proteins. Approximately 20% to 25% of breast cancers are caused by the transmembrane protein receptor known as human epidermal growth factor receptor 2 (HER2), which is encoded by the HER2 gene located on the long arm of chromosome 17. The EGFR family consists of the four HER receptors: HER4, HER3, HER2, and HER (5). Upon HER2 receptor activation, specific tyrosine kinase residues are phosphorylated and signaling proteins are activated upon HER2 receptor activation, leading to the start of downstream signaling processes. The HER2 receptor regulates apoptosis, angiogenesis, cell proliferation, and survival through critical pathways that include mitogen-activated protein kinase (MAPK) and phosphatidylinositol triphosphate kinase (PI3K) signaling mechanisms (6).

In HER2+ breast cancers, HER2 receptor overexpression is known to be a HER2 activation mechanism. HER2-positive breast cancer remains a case study to this day. It is considered a cancer with a poor prognosis due to its high mitotic activity and ability to metastasize easily. However, improved molecular genetic techniques have made it possible to study resistance to trastuzumab (HERCEPTIN) treatment and develop new anti-HER2 targeted therapies. The monoclonal antibody pertuzumab and the tyrosine kinase inhibitor lapatinib specifically target HER2 receptors. The adverse effects of these two chemical and synthetic drugs include alopecia, nausea, vomiting, fatigue, fever, infection, diarrhea,

muscle pain, paresthesia, cognitive disorders, cardiotoxicity, leukemia, and gastrointestinal and dermatological reactions. Several other drugs, such as tamoxifen, raloxifene, toremifene, and fulvestrant, are available for the treatment of breast cancer, but each has limitations that cause irreversible side effects (7). Researchers are searching for other, less toxic, and more natural molecules. Patients are therefore increasingly turning to natural medicine, such as phytotherapy and nutritherapy. There are various benefits to using natural products in food and medicine development, such as their superior chemical diversity, biological potency, structural complexity, and optimized regulation of natural product biosynthesis. Therefore, the goal of this study was to discover a more selective natural compound that targets breast cancer and can be used as a therapeutic agent using *in silico* methods.

## 2. Materials and Methods

### 2.1. Preparation of the protein

The crystal structure of the kinase domain of human HER2 was obtained from the Protein Data Bank (PDB) (<https://www.rcsb.org>) (8), with PDB ID: 3PP0 (9). The structure was downloaded in PDB format and further prepared for the docking process.

### 2.2. Preparation of ligands

Following an extensive literature search, 102 molecules with the potential to interact positively with the ErbB2 receptor tyrosine kinase domain in HER2+ breast cancer were selected. These molecules are derived from plants, microorganisms or food sources.

The ligand codes were obtained from PubChem (<https://pubchem.ncbi.nlm.nih.gov/>) (10), and Zinc Database (<https://zinc.docking.org/>) (11).

### 2.3. Pharmacotoxicity Study of Ligands

To test the toxicity of the plant-derived molecules, we used the PKCSM Database online server (<http://structure.bioc.cam.ac.uk/pkcsml>) (12).

We copied the ligand codes obtained from PubChem and Zinc Database to the pkCSM Database to eliminate toxic ligands based on the following criteria: AMES toxicity, hERG K<sup>+</sup> channel inhibitors toxicity and Hepatotoxicity.

### 2.4. Molecular Docking

Molecular docking was performed using the SwissDock server (<http://www.swissdock.ch/>) (13).

This server allows importing the target molecule, the "tyrosine kinase domain of the HER2 receptor", as well as

the ligands, for the purpose of testing their interactions. The goal is to study the interactions of these two molecules. Investigating the outcomes enables us to identify the binding energy and the hydrogen bonds formed, as well as the amino acids involved in these interactions.

### 2.5. Docking results visualisation

The visualization of the molecular docking results from the SwissDock server is done using the UCSF Chimera software (<https://www.cgl.ucsf.edu/chimera/>) (14).

## 3. Results

### 3.1. Ligand toxicity analysis

Initially, 102 natural compounds were obtained from the databases. These molecules can be found in food sources, such as plants or microorganisms. Some of these compounds were screened for their toxicity based on the predicted mutagenicity screening (AMES Toxicity), HERG K<sup>+</sup> channel inhibitor toxicity, and hepatotoxicity results. The results revealed eight potentially toxic ligands (Table 1). This toxicity could be mitigated by decreasing the administrated dose by 0.558 log mg/kg/day for Genipin, 0.36 log mg/kg/day for Sauchinone, 0.654 log mg/kg/day for Denbinobin, 0.144 log mg/kg/day for Xenognosin, and 0.82 log mg/kg/day for Kaempferol.

### 3.2. Interaction of ligands with HER2

This study investigated the interaction of the 3PP0 protein against 84 ligands. The results are shown in Table 2.

### 3.3. Ligands Interacting With Conserved Residues of the Tyrosine Kinase Domain of EGFR Family Receptors

It notes that there are 47 complexes formed between the ligands and the tyrosine kinase domain of 3PP0, which have the lowest energy scores compared to the other ligands. These complexes form hydrogen bonds with essential residues that are conserved in the EGFR family (Table 2). Therefore, according to interaction energy, the best ligand is Lycopene Table 2. Lycopene from tomato has an interaction energy of -9.82 kcal/mol and no predicted hydrogen bonds, suggesting the existence of other types of bonds by SwissDock (Figure 1). Taking into account what has been cited in the literature, including Met801, which is located in the Adenine region of the ATP binding site, and Cys805, which is located in of hydrophobic pocket II, it has noted that some ligands form interactions with the ATP binding site (Table 2) (15). Compounds that establish a hydrogen bond with the residue Met 801 in the adenine region are as follow:

- **Alpha-Tocopherol**

From sunflower oil has an interaction energy of -7.85 kcal/mol.

- **Isofraxidine**

From the species *Eleutherococcus senticosus*, also known as Siberian ginseng, has an interaction energy of -7.77 kcal/mol.

- **Pyocyanin**

A blue green phenazine molecule produced specifically by the bacterium *Pseudomonas aeruginosa*, has an interaction energy of -7.65 kcal/mol.

- **Sulforaphane**

Which is mainly found in broccoli and cabbage, has an interaction energy of -7.10 kcal/mol.

- **Phloretic acid**

Which belongs to a class of organic compounds found in peanuts and avocados, has an interaction energy of -7.06 kcal/mol.

- **Xenognosin**

Which is present in common peas *Pisum sativum* et legumes, belongs to a class of organic compounds and has an interaction energy of -6.86 kcal/mol.

- **Urocanic acid**

Which is essentially found in the fungus *Hippospongia communis*, has an interaction energy of -6.49 kcal/mol.

- **Sesamol**

Which is found in sesame seed, has an interaction energy of -6.09 kcal/mol.

Other compounds forming hydrogen bonds with cysteine residue 805 in the hydrophobic pocket II are: Syringic acid, found in from olive oil, and Anacardic acid, a component of cashew nuts, have interaction energies (DeltaG) of -6.52 and -7.89 kcal/mol, respectively.

These ligands interact with and form hydrogen bonds with residues Met801 and Cys805 in the ATP binding site of the aforementioned regions. They may have the potential to act as competitive inhibitors by blocking ATP access to its specific site on the tyrosine kinase domain (16, 17). In this study, Anacardic acid is the ligand with the best interaction energy value with the ATP binding site, with a DG of -7.89 kcal/mol (Figure 2).

Two of the 21 ligands, both of which are olive oil, act on the N-lobe of the tyrosine kinase domain. They were selected according to their interactions with residues in the (Cα) helix span residues (729-744).

**Table 1.** Toxicity parameters of some compounds.

Molecules	Mutagenicity	K+ hERG 1	Na + hERG 2	Hepatotoxicity
Genipin	Yes	No	No	No
Sauchinone	Yes	No	No	No
Denbinobin	Yes	No	No	No
Furanodiene	No	No	No	No
Chalcones	No	No	No	No
Isoliquiritoside	No	No	No	No
Xenognosin	Yes	No	No	No
Kaempferol	Yes	No	No	No
Luteolin	Yes	No	No	No
Silibinin	Yes	No	Yes	No
Daidzeine	Yes	No	Yes	No

**Table 2.** Docking results of total ligands with the tyrosine kinase domain obtained by Swiss dock.

Ligands	Residue (s) target(s)	Length of hydrogen bond (Å)	Interaction energy (kcal/mol)
Crocetin	ALA 706	3.011	-9.46
	ALA 706	3.324	-9.46
Secoisolariciresinol diglucoside	GLU 757	1.841	-8.41
Lycopene	-----	No hydrogen bond	-9.82
P-coumaric acid	-----	No hydrogen bond	-8.57
Curcumin	-----	No hydrogen bond	-8.46
Pomiferin	-----	No hydrogen bond	-8.08
Formononetin	-----	No hydrogen bond	-8.07
Rosmarinic acid	-----	No hydrogen bond	-7.83
3,4-Dihydroxybenzoic	GLY 737	1.915	-6.22
4 P-hydroxybenzoic acid 1	SER 779	2.213	-6.88
4 P-hydroxybenzoic acid 2	-----	No hydrogen bond	-6.21
Gallic acid	VAL 777	2.517	-6.25
Gentisic acid	-----	No hydrogen bond	-6.93
Syringic acid	CYS 805	3.096	-6.51
Vanillic acid	VAL 777	2.191	-6.20
Catechines	VAL 777	3.187	-6.82
Epicatechines	GLN 943	1.819	-6.74
Biochanine A	LEU 726	3.347	-6.67
Ergostane	-----	No hydrogen bond	-6.18
Glycitein	-----	No hydrogen bond	-6.37
Daidzeine	VAL 777	2.114	-6.61
Genistein	CYS 947	1.995	-7.54
Malvidin	VAL 777	3.031	-7.32
Delphinidine	-----	No hydrogen bond	-6.70
Cyanidin	GLN 709	2.003	-7.00
	GLN 709	1.929	-7.00
Acetoxypinoresinol	-----	No hydrogen bond	-7.29
Pinoresinol	SER 728	2.523	-7.80
Hydroxytyrosol	ARG 849	2.215	-6.91
Tyrosol	ARG 849	2.129	-6.36
Secoisolariciresinol	-----	No hydrogen bond	-7.49
Enterodiol	PRO 945	2.169	-6.63
Enterolactone	-----	No hydrogen bond	-7.51
Capsaicin	-----	No hydrogen bond	-7.62
CAPE	-----	No hydrogen bond	-6.46
Caffeic-acid-phenethyl ester	-----	No hydrogen bond	-6.46
$\alpha$ -Linolenic acid	SER 728	3.160	-7.69
Chlorogenic acid	GLN 943	2.140	-6.96
Ferulic acid	-----	No hydrogen bond	-7.37

<b>Gingerol</b>	-----	<b>No hydrogen bond</b>	<b>-7,27</b>
<b>Petunidin</b>	-----	No hydrogen bond	-7,03
<b>Pelagronidine</b>	GLY 778	2,052	-6,38
<b>Homocastasterone</b>	ASP838	2.716	-7.44
<b>Cafeic</b>	LEU1000	2.044	-6.71
<b>Sinapic</b>	CYS 805	2.052	-7.40
<b>3-Hydroxybenzoic</b>	-----	No hydrogen bond	-6.68
<b>O-coumaric acid</b>	-----	No hydrogen bond	-6.05
<b>Diindolylmethane</b>	-----	No hydrogen bond	-7,31
<b>Naringenine</b>	GLN943	1.841	-6.65
<b>Indol 3-carbinol</b>	-----	No hydrogen bond	-6.13
<b>Kaempferol</b>	ASP 863	3.572	-6.88
<b>Dihydroresveratrol</b>	-----	No hydrogen bond	-7.15
<b>Resveratrol</b>	-----	No hydrogen bond	-6.51
<b>Sulforaphane</b>	MET 801	3.708	-7.10
<b>Myricetin</b>	-----	No hydrogen bond	-7.03
<b>Quercetin</b>	ALA706	2.130	-7.28
	VAL 777	3.491	
<b>Apigenin</b>	CYS 947	2.064	-7.55
<b>Luteolin</b>	ALA 706	2.132	
	VAL 777	2.247	-7.92
<b>Fisetin</b>	VAL777	3.336	-6.55
<b>Sauchinone</b>	-----	No hydrogen bond	-6.83
<b>Denbinobin</b>	-----	No hydrogen bond	-7.01
<b>Furanodiene</b>	-----	No hydrogen bond	-6.82
<b>Chalcone</b>	-----	No hydrogen bond	-7.19
<b>Lupane</b>	-----	No hydrogen bond	-6.77
<b>Genipin</b>	VAL 777	2.696	-6.50
	VAL 777	3.142	
<b>Opium</b>	VAL777	2.054	-6.70
<b>Pyocyanin</b>	MET801	2.162	-7.65
<b>Ginsenosol</b>	ALA706	2.131	-6.34
<b>Menthol</b>	VAL777	2.329	-6.10
<b>Urocanic acid</b>	MET801	2.182	-6.49
<b>Anthranilic acid</b>	ALA706	2.410	
	ALA706	2.177	-7.54
<b>Anacardic acid</b>	CYS805	2.049	-7.89
	VAL777	2.073	
<b>Diosmetin</b>	GLN709	2.348	-6.60
<b>Khahalalide D</b>	THR759	2.385	-7.39
<b>Alpha-tocopherol</b>	MET801	2.433	-7.85
<b>Beta-carotene</b>	-----	No hydrogen bond	-8.58
<b>Choline</b>	CYS802	2.442	-6.30
<b>Sesamol</b>	MET801	2.612	-6.09
<b>Silibinin</b>	VAL777	2.197	-7.16
	LEU711	2.546	
<b>Xanthoxylin</b>	VAL777	2.509	-6.26
	MET801	2.084	
<b>Isofraxidin</b>	VAL777	2.117	-7.77
	MET801	1.939	
<b>Phloretic acid</b>	VALL777	2.034	-7.06
	GLN990	2.118	
<b>Indole-3-carboxylic acid</b>	PHE731	2.003	-7.81
	GLN990	2.077	
<b>Garlic</b>	-----	No hydrogen bond	-6.69
<b>Xenognosin</b>	MET801	2.156	-6.86



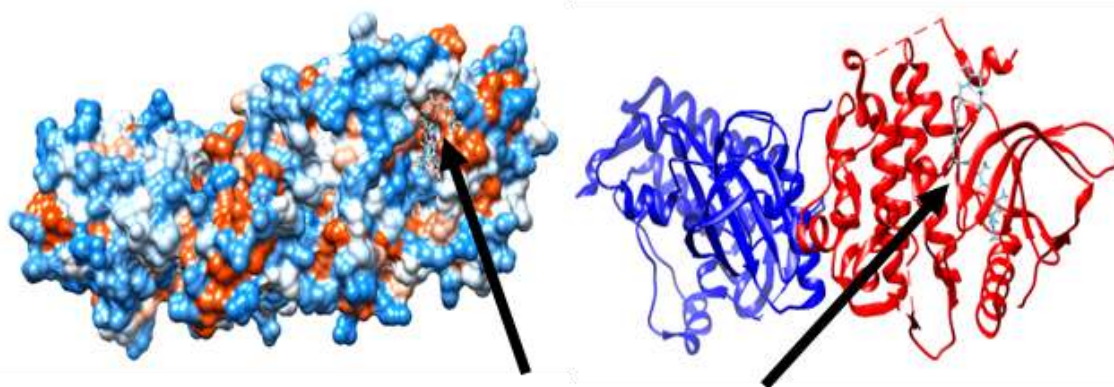


**Figure 1.** Three-dimensional illustration of the 3PP0-Lycopene complex using the molecular surface (A) and the ribbon model (B)

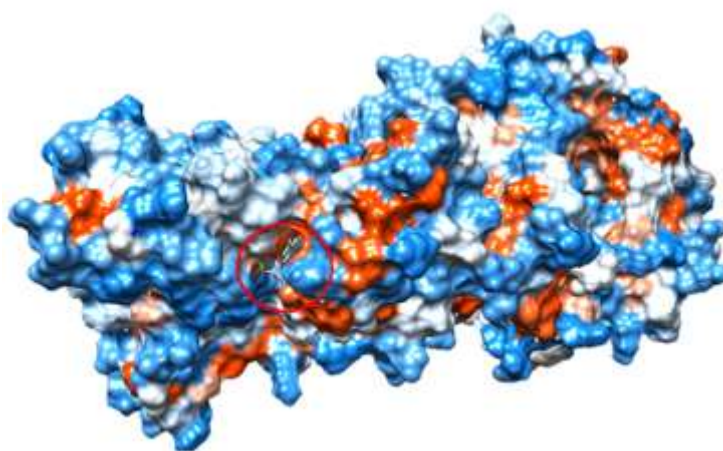


**Figure 2.** Three-dimensional illustration of the 3PP0 -Anacardic acid complex using the molecular surface.

3,4-Dihydroxybenzoic acid has an interaction energy of -6.22 kcal/mol and forms a hydrogen bond with the residue Gly737.

Sinapic acid has an interaction energy of -7.40 kcal/mol and forms a hydrogen bond with the residue Gly732.

Both ligands form hydrogen bonds:

3,4-dihydroxybenzoic acid forms a bond with residue Gly737 and Sinapic acid forms a bond with residue Gly732 within the (C $\alpha$ ) helix. This could destabilize the active open conformation of the activation loop (C-helix-in-DFG-in) and prevent ATP substrate binding to its specific site. It could also block of trans-autophosphorylation of the activation loop, which would maintain its inactive conformation. The ATP binding groove would no longer be accessible, and the tyrosines of the C-terminal tail would not be phosphorylated by the catalytic loop. This induces blockage of the downstream signaling cascade (18). In the present study, Sinapic acid

is the target with the best interaction energy value acting on the N-lobe (C $\alpha$ -helix), with a DG of -7.40 kcal/mol (Figure 3).

Three of these 47 ligands act on the A-loop of the C-lobe of the tyrosine kinase domain. According to the literature, the 20-30 residue sequence of the activation loop (Asp831-Val852 in the EGFR family) contains the conserved base DFG motif (Asp831-Phe-Gly833 in the EGFR family) and extends to an APE (Ala-Pro-Glu) motif also contains the Tyr845 residue, which is one of the target tyrosines for autophosphorylation by the catalytic loop (16-18).

#### • Tyrosol and Hydroxytyrosol

Found in olive oil, have interaction energies of -6.36 and -6.91 kcal/mol, respectively. Each compound forms a hydrogen bond with an estimated length of 2.129 Å for tyrosol and 2.215 Å for hydroxytyrosol with residue Arg849 of chain A for tyrosol and chain B for hydroxytyrosol.

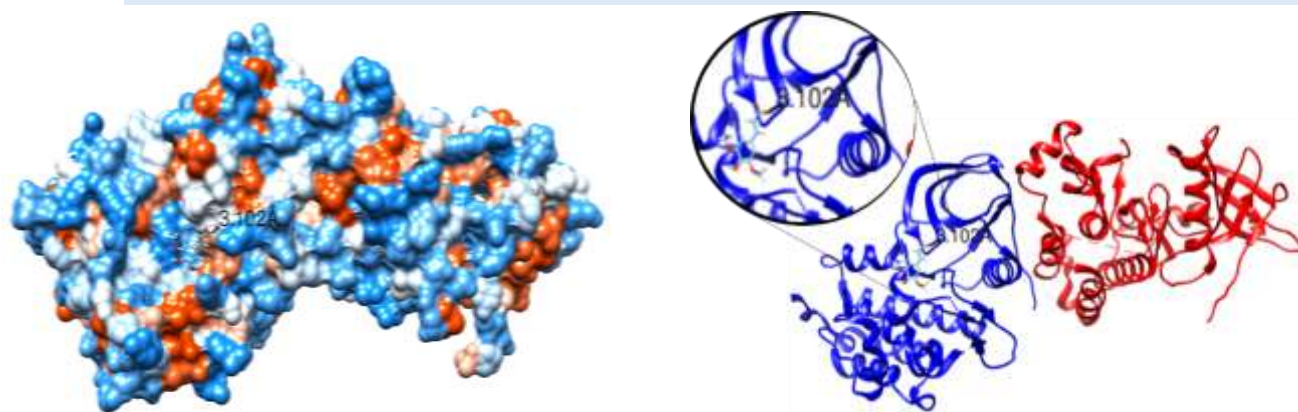


**Figure 3.** Three-dimensional illustration of the 3PP0-Sinapic acid complex using the molecular surface (A) and the ribbon model (B).

### • Homocasterone

Found in beans, has an interaction energy of -7.44 kcal/mol and forms a strong hydrogen bond with Asp838 of the A chain, with an estimated length of 2.716Å.

Thus, the ligand Homocasterone forms a hydrogen bond with the residue Asp838, the ligands Tyrosol and Hydroxytyrosol each form a hydrogen bond with the residue Arg849 of the activation loop. These ligands can therefore block its activation and passage between conformations:

Inactive (C-helix-out-DF Gout), partially inactive (C-helix-in-DF Gout), and finally active (C-helix-in-DF Gin). This effect occurs by sequestering the trans-autophosphorylation of these tyrosine residues to phosphotyrosines by the catalytic loop after dimerization. Consequently, the ATP binding groove is inaccessible, preventing trans phosphorylation of the C-terminal tail and the recruitment of adaptor proteins (16-20).

This study shows that the ligand with the best interaction energy value that acts on loop A and lobe-C is Homocasterone with a DG of -7.44 kcal/mol (Figure 4).

Other ligands were selected according to their interactions with the following residues in the hydrophobic region of ErbB2: Val773, Met774, Gly776, Val777, Gly778, and Val782 in the  $\alpha$ C- $\beta$ 4 loop (21). For example, Pelagronidin from grapes forms a hydrogen bond with Gly778. \*Sixteen of these ligands form a hydrogen bond with the same Val777 residue (Table 2):

*Vanillic acid* from olive oil, *Catechin* from blackcurrant, *Malvidin* from grapes, *Fisetin* from strawberries and apples, *Genipin* from *Gardenia Jasminoides Ellis* species, *Opuim*, *Gallic acid*, *Menthol* from peppermint and tea, *Diosmetin* from sage and thyme, *Quercetin* from red onions or buckwheat, *Luteolin* from green peppers, olive oil and carrots, *Xanthoxylin* from fats,

oils, herbs and spices, Isofraxidin Phloretic acid, *Silibinin* extracted from the milk thistle flowers and *Daidzein* present in flax seeds. These two ligands have better interaction energy and strong bonds, but according to the Pharmacotoxicity tests, these two molecules are mutagenic and toxic. These ligands form hydrogen bonds with residues (valine 777), which belong to the hydrophobic region of ErbB2 ( $\alpha$ C- $\beta$ 4 loop). These residues interact with the activation loop and can destabilize conformational changes from the inactive conformation (C-helix-out-DFGout) to the partially inactive conformation (C-helix-in-DFGout) and finally to the active conformation (C-helix-in DFGin). This occurs by sequestering trans autophosphorylation by the catalytic loop after dimerization. Thus, the ATP binding groove remains covered, there is no trans autophosphorylation of the C-terminal tail, and therefore, no recruitment of adaptor proteins (21).

This result indicated that Luteolin, with a DG of -7.92 kcal/mol, is the ligand with the best interaction energy value that interacts with the residues of the hydrophobic region in the loop ( $\alpha$ C- $\beta$ 4) (Figure 5).

According to the literature, the residues of the hydrophobic region of loop A are Iso861, Thr862, Phe864, Leu866 and Leu869. The interaction between the two active and inactive conformations, which takes place between Ser783 with in the hydrophobic region of ErbB2 ( $\alpha$ C- $\beta$ 4 loop) and residue Iso861 of loop A, allows the interaction between the latter and the  $\alpha$ C- $\beta$ 4 loop (21).

The ligands Vanillic acid, Catechins, Malvidin, Fisetin, Genipin, Pelagronidin and 4 p-hydroxybenzoic acid form hydrogen bonds with residues belonging to the hydrophobic region of ErbB2 ( $\alpha$ C- $\beta$ 4 loop) and interact

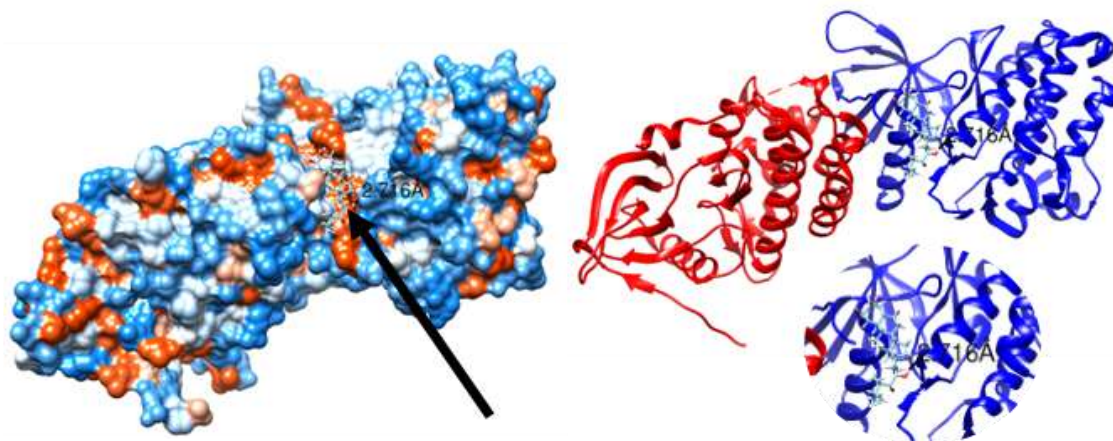


**Figure.4:** Three-dimensional illustration of the 3PP0 – Homocasterone complex using the molecular surface (A) and the ribbon model (B).

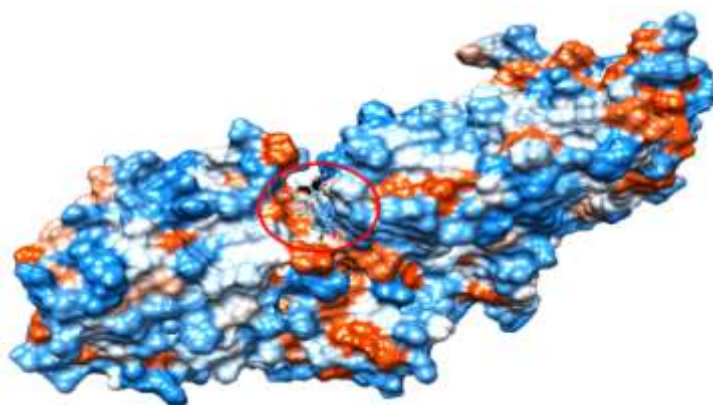


**Figure 5.** Three-dimensional illustration of the 3PP0 -Luteolin complex using the molecular surface.

with the activation loop. These ligands can destabilize conformational changes from the inactive conformation (C-helix-out-DFGout) to the partially inactive conformation (C-helix-in-DFGout) and finally to the active conformation (C-helix-in-DFGin). This occurs by sequestering trans autophosphorylation by the catalytic loop after dimerization. Consequently, the ATP-binding groove remains covered, preventing trans autophosphorylation of the C-terminal tail and the recruitment of adaptor proteins (21).

In this study, malvidin with a DG of -7.32 kcal/mol, is the ligand that with the best interaction energy value and interacts with residues in the hydrophobic region (in the  $\alpha$ - $\beta$ 4 loop) (Figure 6).

The remaining five ligands were selected according to their interactions with residues between the tyrosines of the C-terminal tail (Tyr874, Tyr992, Tyr1048, Tyr1068, Tyr1086, Tyr1101, and Tyr1173) (Table 2) (17).

The aforementioned tyrosines correspond to residues trans-autophosphorylated by the catalytic loop. Therefore, ligands that form hydrogen bonds with residues, that lie between these tyrosines, such as Epicatechin and Naringenin with residue Gln943, Apigenin with residue Cys947, Genistein with residue Cys947, may be susceptible to sequestration of the interaction between the C-terminal tail and the catalytic loop. Therefore the tyrosines will not be trans-autophosphorylated, the adaptor proteins will not be recruited (17).

Apigenin has the best interaction energy value with residues between the tyrosines of the C-terminal tail, with a DG of -7.55 kcal/mol (Figure 7).

#### 3.4. Ligands Interacting with Specific Residues of the HER-2 Receptor Tyrosine Kinase Domain

One ligand acts on the P-loop of the N-lobe of the tyrosine kinase domain. Non-conserved ligands specific to HER2 were selected based on their interaction with



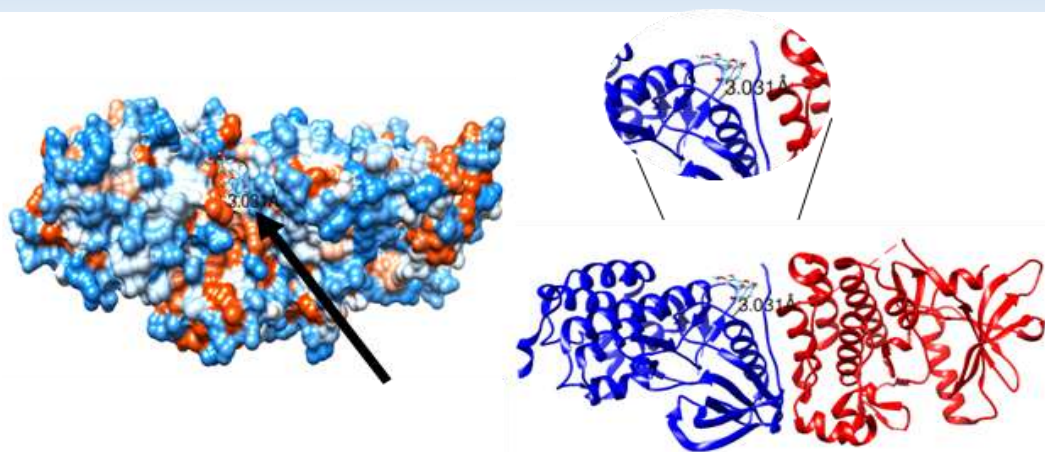


**Figure 6.** Three-dimensional illustration of the 3PP0 -Malvidin complex using the molecular surface (A) and the ribbon model (B).

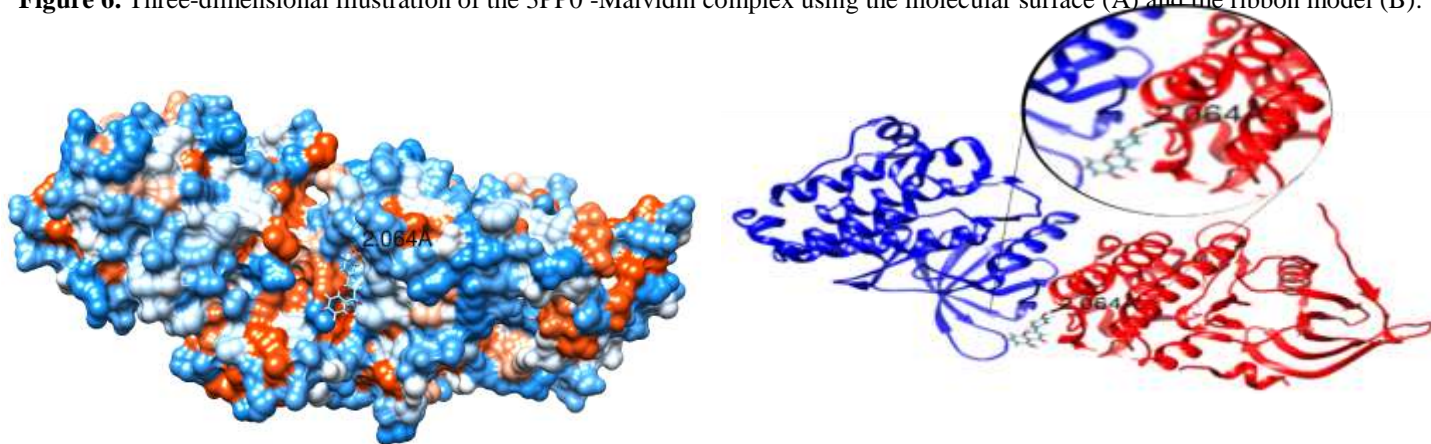


**Figure 7.** Three-dimensional illustration of the 3PP0- Apigenin complex using the molecular surface (A) and the ribbon model (B).

residues from residue Leu726 to Val734 (9). Pinoresinol, found in olive oil, has an interaction energy of -7.48 kcal/mol and forms a strong hydrogen bond whose length, estimated at 2.613 Å with the residue Ser728 (Figure 8).

This ligand forms a hydrogen bond with the P-loop, which can destabilize the open active conformation of the activation loop (C-helix-in-DFGin) and prevent binding of the ATP substrate to its specific site. This blocks the downstream signaling cascade (16).

One ligand that acts on the C-terminal tail of the non-conserved tyrosine kinase domain in the EGFR family was selected based on its interaction with the residues extending from residue Pro999 to Leu1009 and was specific for HER2. The caffeic acid in olive oil has an interaction energy of -6.71 kcal/mol and forms a hydrogen bond with the residue Leu1000, estimated to be 2.044 Å long (9).

Two ligands acting on the P-loop of the N-lobe of the tyrosine kinase domain were selected according to their interaction with residues in the sequence extending from Leu726 to Val734 (9). Biochanin A from Soybean has an interaction energy of -6.67 kcal/mol with Leu 726, and  $\alpha$ -Linolenic acid from soybean has an interaction energy of -7.69 kcal/mol and forms a strong hydrogen bond with an estimated length of 3.160 Å with the residue Ser728.

The  $\alpha$ -helix and the P-loop are in close proximity and interact with ATP required for trans-autophosphorylation in the ATP-binding site (9, 17). The ligands such as Biochanin A, Pinoresinol and  $\alpha$ -Linolenic acid form hydrogen bonds with the P-loop and can destabilize the active, open conformation of the activation loop (C-helix-in-DFGin), thus preventing no ATP substrate binding at its specific site and inducing blockage of the downstream signaling cascade (18).

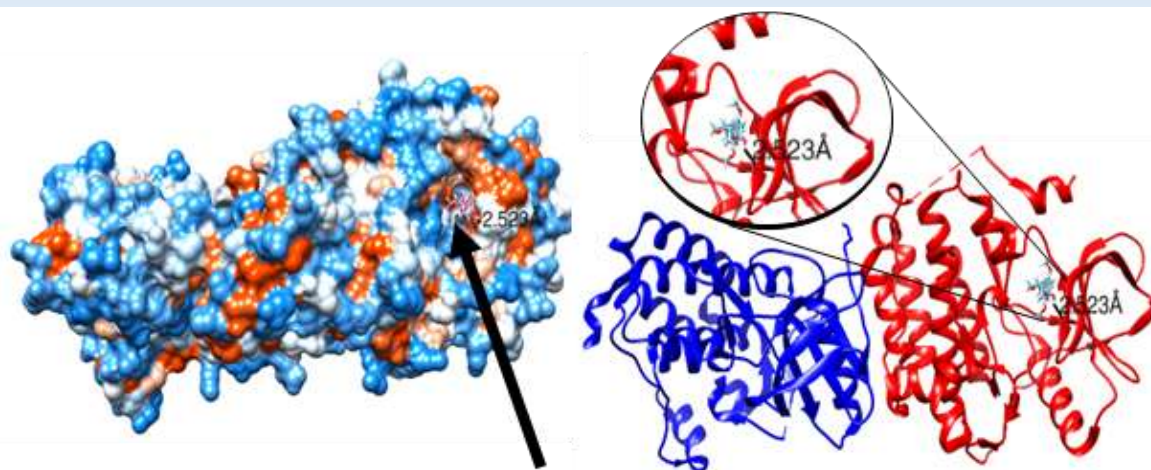


**Figure 8.** Three-dimensional illustration of the 3PP0-Pinoresinol complex using the molecular surface (A) and the ribbon model (B).

The ligand that has the best interaction energy value with the N-lobe P-loop residues specific for HER2 is  $\alpha$ -Linolenic with a DG of -7.69 kcal/mol (Figure 9).

The remaining ligand that acts on the helix ( $C\alpha$ ) of the N-lobe of the tyrosine kinase domain was selected according to its interaction with the residues in the stretch extending from Pro761 to Ala775.

One ligand acts on the C-lobe activation loop of the HER2 receptor-specific tyrosine kinase domain was selected based on their interaction with residues spanning from Asp863 to Val884, including the DFG motif (from residue Asp863 to residue Gly865). Kaempferol Present an interaction energy of -6.88 Kcal/mol and forms a hydrogen bond with the residue ASP863, estimated at 3.572 Å (Figure 10).

### 3.5. Visualization of Lapatinib Docking Results with 3PP0

Lapatinib is a ligand which is used as a chemical treatment in HER2+ breast cancer that is specific for inhibiting protein tyrosine kinase signaling pathways (22). Our findings indicate that it has an interaction energy of -7.58 kcal/mol and forms a hydrogen bond whose length is estimated at 2.303Å with the Val777 residue of the A chain. Lapatinib, therefore, interacts with the residues of the hydrophobic region of ErbB2 in the  $\alpha$ C- $\beta$ 4 loop (Figure 11A).

### 3.6. Comparison of the Two Ligands Lapatinib and Quercetin

The quercetin found in red onions or buckwheatsssshas an interaction energy of -7.28 Kcal/mol and forms a hydrogen bond with the residue Val777 ,whose length is estimated at 2.130 Å (Figure 11A).

Based on the visualizing the results of the two ligands, Lapatinib and quercetin (the former a modified chemical ligand and the latter a natural ligand primarily found in red

onions), it appears that each forms a hydrogen bond of different lengths: 2.303Å for Lapatinib and of 2.130Å for a quercetin, both with the residue valine777 in the hydrophobic region (in the  $\alpha$ C- $\beta$ 4 loop).The interaction energies are -7.58kcal/mol for Lapatinib and-7.28kcal/mol for quercetin. Lapatinib certainly has a better interaction energy, but it is a chemical compound with side effects. Quercetin,on the other hand, has other beneficial effects on health in addition to its possible inhibition of 3PP0.

### 3.5. Visualization of Lapatinib Docking Results with 3PP0

Lapatinib is a ligand which is used as a chemical treatment in HER2+ breast cancer that is specific for inhibiting protein tyrosine kinase signaling pathways (22). Our findings indicate that it has an interaction energy of -7.58 kcal/mol and forms a hydrogen bond whose length is estimated at 2.303Å with the Val777 residue of the A chain. Lapatinib, therefore, interacts with the residues of the hydrophobic region of ErbB2 in the  $\alpha$ C- $\beta$ 4 loop (Figure 11A).

### 3.6. Comparison of the Two Ligands Lapatinib and Quercetin

The quercetin found in red onions or buckwheatsssshas an interaction energy of -7.28 Kcal/mol and forms a hydrogen bond with the residue Val777 ,whose length is estimated at 2.130 Å (Figure 11A).

Based on the visualizing the results of the two ligands, Lapatinib and quercetin (the former a modified chemical ligand and the latter a natural ligand primarily found in red onions), it appears that each forms a hydrogen bond of different lengths: 2.303Å for Lapatinib and of 2.130Å for a quercetin, both with the residue valine777 in the hydrophobic region (in the  $\alpha$ C- $\beta$ 4 loop). The interaction energies are -7.58kcal/mol for Lapatinib and-7.28kcal/mol for quercetin. Lapatinib certainly has a better interaction



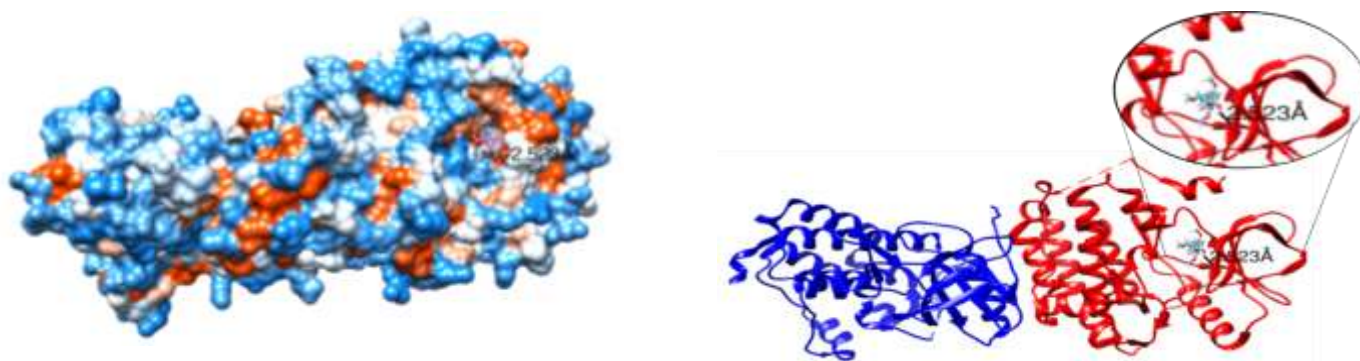


**Figure 9.** Three-dimensional illustration of the 3PP0 -  $\alpha$ -Linolenic complex using the molecular surface (A) and the ribbon model (B).

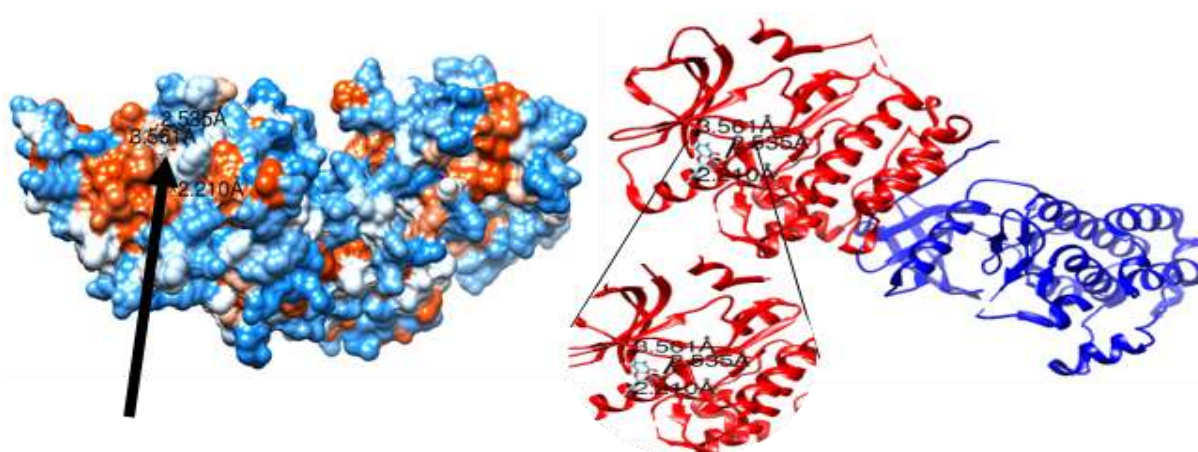


**Figure 10.** Three-dimensional illustration of the 3PP0 - Kaempferol complex using the molecular surface (A) and the ribbon model (B).

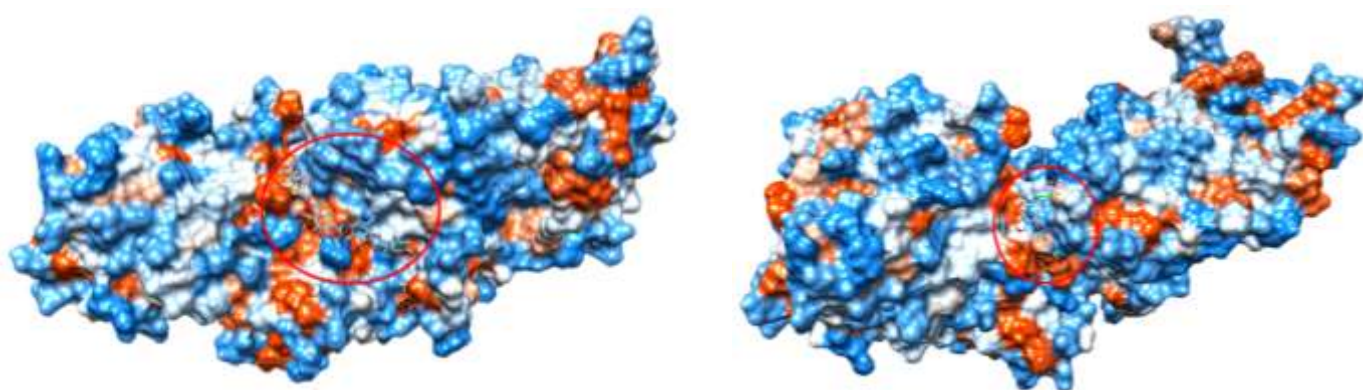


**Figure 11.** Three-dimensional illustration of the 3PP0 - Lapatinib (A) and 3PP0 - meletin (B) using the molecular surface

energy, but it is a chemical compound with side effects. Quercetin, on the other hand, has other beneficial effects on health in addition to its possible inhibition of 3PP0.

#### 4. Discussion

Indeed, quercetin, also known as vitamin P, is a food-derived compound and a bioflavonoid found in the pigments of colored fruits and vegetables. These include red onions, spinach, turmeric, apples, red grapes, carrots, berries, broccoli, green tea, lovage, chocolate or red wine. As a natural antioxidant, quercetin helps fight against oxidative stress by capturing and blocking the activity of free radicals and inhibiting the oxidation of lipids. Quercetin is also involved in regulation of signaling pathways, cell cycle proliferation and the immune response. In summary, investigating *in silico* before proceeding to the experimental stage can save a great deal of time and money. *In silico* technologies can predict a number of ADMET factors, toxicological effects, and likely active medication. In this study, the oral bioavailability of drugs was predicted using several prediction methodologies, which could lead to the development of safer, innovative pharmaceuticals. After analyzing the screening and molecular docking studies, we found that many natural products could be used as potential HER2 antagonists to treat of breast cancers. Additional wet-lab research is necessary to further evaluate these selected compounds.

#### Acknowledgment

None.

#### Authors' Contribution

Conceived and designed experiments: N. L.

Conducted experiments: N. L.

Analyzed data: N. L, N. M, S KT.

Wrote the paper: N. L.

#### Ethics

In this article, the authors have observed all ethical points, including those related to plagiarism, double publication, data distortion and data manipulation.

#### Conflict of Interest

The author declares no known competing interests.

#### Grant Support

This study

#### Data Availability

The data supporting the findings of this study are available upon request from the corresponding author.

#### References

1. Domeyer P-RJ, Sergeantanis TN. New insights into the screening, prompt diagnosis, management, and prognosis of breast cancer. *Journal of Oncology*. 2020;2020:8597892.
2. Dai X, Xiang L, Li T, Bai Z. Cancer hallmarks, biomarkers and breast cancer molecular subtypes. *Journal of cancer*. 2016;7(10):1281.
3. Hsu JL, Hung M-C. The role of HER2, EGFR, and other receptor tyrosine kinases in breast cancer. *Cancer and Metastasis Reviews*. 2016;35:575-88.
4. Maennling AE, Tur MK, Niebert M, Klockenbring T, Zeppernick F, Gattenlöhner S, et al. Molecular targeting therapy against EGFR family in breast cancer: progress and future potentials. *Cancers*. 2019;11(12):1826.
5. Schlam I, Swain SM. HER2-positive breast cancer and tyrosine kinase inhibitors: the time is now. *NPJ breast cancer*. 2021;7(1):56.
6. Furrer D, Paquet C, Jacob S, Diorio C. The human epidermal growth factor receptor 2 (HER2) as a prognostic and predictive biomarker: Molecular insights into HER2 activation and diagnostic implications. *Cancer prognosis*. 2018;5:11-21.
7. Sharma D, Kumar S, Narasimhan B. Estrogen alpha receptor antagonists for the treatment of breast cancer: a review. *Chemistry Central Journal*. 2018;12:1-32.
8. Berman HM, Westbrook J, Feng Z, Gilliland G, Bhat TN, Weissig H, et al. The protein data bank. *Nucleic acids research*. 2000;28(1):235-42.
9. Aertgeerts K, Skene R, Yano J, Sang B-C, Zou H, Snell G, et al. Structural analysis of the mechanism of inhibition and allosteric activation of the kinase domain of HER2 protein. *Journal of Biological Chemistry*. 2011;286(21):18756-65.
10. Kim S, Chen J, Cheng T, Gindulyte A, He J, He S, et al. PubChem 2023 update. *Nucleic acids research*. 2023;51(D1):D1373-D80.
11. Irwin JJ, Sterling T, Mysinger MM, Bolstad ES, Coleman RG. ZINC: a free tool to discover chemistry for biology. *Journal of chemical information and modeling*. 2012;52(7):1757-68.



12. Pires DE, Blundell TL, Ascher DB. pkCSM: predicting small-molecule pharmacokinetic and toxicity properties using graph-based signatures. *Journal of medicinal chemistry*. 2015;58(9):4066-72.
13. Grosdidier A, Zoete V, Michielin O. SwissDock, a protein-small molecule docking web service based on EADock DSS. *Nucleic acids research*. 2011;39(suppl\_2):W270-W7.
14. Pettersen EF, Goddard TD, Huang CC, Couch GS, Greenblatt DM, Meng EC, et al. UCSF Chimera—a visualization system for exploratory research and analysis. *Journal of computational chemistry*. 2004;25(13):1605-12.
15. Yim-Im W, Sawatdichaikul O, Semsri S, Horata N, Mokmak W, Tongsima S, et al. Computational analyses of curcuminoid analogs against kinase domain of HER2. *BMC bioinformatics*. 2014;15:1-13.
16. Aller P. Etude du domaine transmembranaire de recepteur tyrosine kinase dans un environnement membranaire. Aspects structuraux et mecanistiques explores par dynamique moleculaire: Université d'Orléans; 2004.
17. Martin-Fernandez ML, Clarke DT, Roberts SK, Zanetti-Domingues LC, Gervasio FL. Structure and dynamics of the EGF receptor as revealed by experiments and simulations and its relevance to non-small cell lung cancer. *Cells*. 2019;8(4):316.
18. Modi V, Dunbrack Jr RL. Defining a new nomenclature for the structures of active and inactive kinases. *Proceedings of the National Academy of Sciences*. 2019;116(14):6818-27.
19. Vijayan R, He P, Modi V, Duong-Ly KC, Ma H, Peterson JR, et al. Conformational analysis of the DFG-out kinase motif and biochemical profiling of structurally validated type II inhibitors. *Journal of medicinal chemistry*. 2015;58(1):466-79.
20. Klug LR, Kent JD, Heinrich MC. Structural and clinical consequences of activation loop mutations in class III receptor tyrosine kinases. *Pharmacology & therapeutics*. 2018;191:123-34.
21. Shih AJ, Telesco SE, Radhakrishnan R. Analysis of somatic mutations in cancer: molecular mechanisms of activation in the ErbB family of receptor tyrosine kinases. *Cancers*. 2011;3(1):1195-231.
22. Ulrich L, Okines AF. Treating advanced unresectable or metastatic HER2-positive breast cancer: a spotlight on tucatinib. *Breast Cancer: Targets and Therapy*. 2021;361-81.